Carrier envelope offset frequency of a doubly resonant, nondegenerate, mid-infrared GaAs optical parametric oscillator

Kevin F. Lee,[1,*] Jie Jiang,[1] C. Mohr,[1] J. Bethge,[1] M. E. Fermann,[1] Nick Leindecker,[1,2] Konstantin L. Vodopyanov,[2] Peter G. Schunemann,[3] and I. Hartl[1]

[1]*IMRA America, Inc., 1044 Woodridge Avenue, Ann Arbor, Michigan 48105, USA*

[2]*E.L. Ginzton Laboratory, Stanford University, Stanford, California 94305, USA*

[3]*BAE Systems, P.O. Box 868 Nashua, New Hampshire 03063, USA*

**Corresponding author: klee@imra.com*

Received January 21, 2013; revised March 6, 2013; accepted March 7, 2013; posted March 7, 2013 (Doc. ID 183820); published April 1, 2013

We measure the carrier envelope offset (CEO) frequency of the mid-infrared frequency comb (wavelength tunable between 3 and 6 μm) from a doubly resonant nondegenerate synchronously pumped optical parametric oscillator (SPOPO) as a function of the CEO frequency of the Tm-fiber pump laser. We show that the CEO frequency of the SPOPO signal wave is a linear function of the CEO frequency of the pump laser, with a slope determined by the signal to pump center-frequency ratio. © 2013 Optical Society of America

OCIS codes: 190.4970, 190.4975.

Frequency combs, coherently stabilized trains of laser pulses, are important tools for metrology [1] and spectroscopy [2]. Mid-infrared frequency combs are an ideal tool for molecular spectroscopy, since they can probe the molecular fingerprint spectral region [3], leading to a push in laser technology to provide these sources [4]. One approach is to use a synchronously pumped optical parametric oscillator (SPOPO) to split short wavelength pump photons into longer wavelength mid-infrared photons using a nonlinear crystal in an optical cavity [5]. Much progress has been made recently in generating mid-infrared frequency combs by optical parametric oscillation, such as a 1.5 W mid-infrared frequency comb [6] and an ultrabroadband mid-infrared doubly resonant SPOPO operating at degeneracy [7].

Many frequency comb spectroscopy methods require a narrow comb tooth linewidth as well as stabilized repetition frequency (or comb spacing) f_{rep} and offset frequency f_{ceo}. A SPOPO automatically inherits f_{rep} through its pump wave (p), leaving signal (s) and idler (i) offset frequencies f^{s}_{ceo} and f^{i}_{ceo} to be determined and controlled. In singly resonant SPOPOs, f_{ceo}-control is typically done by slight SPOPO cavity length detuning, which results in a shift of signal and idler spectrum and therefore a f_{ceo} shift [6,8,9].

The situation is different in a doubly resonant SPOPO, since the SPOPO only oscillates in a discrete set of cavity length detunings with widely different output spectra [10]. In the degenerate case, signal and idler are indistinguishable and it was shown by Wong *et al.* [11] that here $f^{s,i}_{\mathrm{ceo}}$ is automatically locked to f^{p}_{ceo}, such that $\Delta f^{s,i}_{\mathrm{ceo}}/\Delta f^{p}_{\mathrm{ceo}} = 1/2$.

Nondegenerate operation has the potential of extending the OPO tuning range all the way to the IR transparency cutoff of the nonlinear crystal. However, the $f^{s}_{\mathrm{ceo}} = f^{i}_{\mathrm{ceo}}$ condition for automatic $f^{s,i}_{\mathrm{ceo}}$ stabilization is no longer valid and the SPOPO's carrier envelope offset (CEO) stability is not obvious. Here we show, that in the nondegenerate case, f^{s}_{ceo} and f^{i}_{ceo} are locked to the pump wave.

Our setup is similar to that in [10]. The SPOPO is a 3 m ring cavity, with a 0.5 mm long orientation-patterned gallium arsenide (OP-GaAs) gain crystal with a 60.5 μm reversal period placed at Brewster angle. The pump source is a Tm-fiber frequency comb producing 70 fs pulses, centered at 2 μm, with a comb spacing of 98.56 MHz, and an average power of 400 mW. The pump is coupled into the cavity by a dielectric mirror that transmits the 2 μm pump, and reflects from 3 to 6 μm. The pump is then focused into the OP-GaAs crystal by the resonator's spherical gold mirror. The cavity is designed to be resonant for both the signal and idler. We use a CaF_2 wedge of about half a millimeter thickness at Brewster's angle for second-order dispersion compensation. Our output is the light that leaves the cavity from the imperfect reflection of the input coupler with a power of a few milliwatts. The output power can be increased easily by tilting the CaF_2 wedge for use as an output coupler, similar to [10].

To maintain oscillation, the SPOPO cavity length is actively stabilized by a dither lock using a fast piezoelectric transducer (PZT) for cavity length dithering at 3.3 kHz, while a PbSe detector measures scattered mid-infrared light. An electronic stabilization circuit maximizes the signal on the PbSe detector by feedback control to a slow PZT for cavity-length control. As usual for a doubly resonant SPOPO, there exists a series of resonant cavity lengths producing different output spectra, as shown in Fig. 1. The entire tuning range of the SPOPO spans one octave from 3 to 6 μm.

Our experimental approach for testing the offset frequency of the SPOPO is sketched in Fig. 2. In our scheme we require a fully stabilized frequency comb for the pump laser. We achieve this as described in [12]. In brief, we amplify part of the Tm-fiber oscillator's output and generate octave-spanning supercontinuum in a highly nonlinear fiber. We use a spectral slice around 1.5 μm of the supercontinuum for generating a beat signal f^{p}_{beat} with a reference laser and the spectral edges of the supercontinuum for self-referenced offset frequency f^{p}_{ceo} detection. Both f^{p}_{beat} and f^{p}_{ceo} are phase-locked to RF

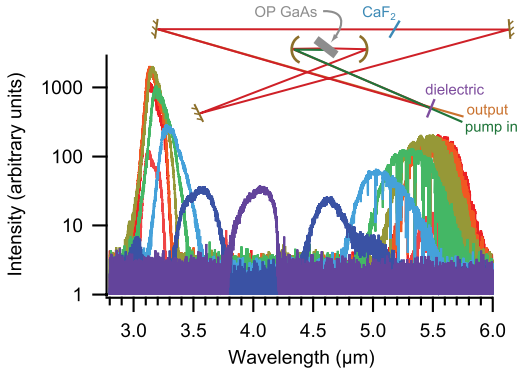

Fig. 1. (Color online) Schematic of the SPOPO cavity, and measured SPOPO spectra for different cavity lengths. In this case, the cavity was optimized for a large signal–idler splitting. At long wavelengths, residual atmospheric absorption lines are visible.

references by feedback to the Tm-fiber oscillator's cavity length and pump power, respectively. The Tm-fiber comb is then fully stabilized, and its comb spacing f_{rep} follows the reference laser's frequency ν_{ref} by the comb equation $f_{\mathrm{rep}} = (\nu_{\mathrm{ref}} \pm f^{p}_{\mathrm{ceo}} \pm f^{p}_{\mathrm{beat}})/n_{\mathrm{ref}}$, where the integer n_{ref} is the index of the Tm-fiber comb line beating with the reference laser, with $n_{\mathrm{ref}} \approx 2 \cdot 10^{6}$. The reference laser was a single-frequency diode laser (Redfern Integrated Optics) with $c/\nu_{\mathrm{ref}} = 1565$ nm, 3 kHz linewidth, and about 4 MHz drift over 3 h (Fig. 4).

A beat experiment between the SPOPO's signal comb and our reference laser allows us to measure the offset frequency of the signal comb f^{s}_{ceo}. We first select a SPOPO resonance at the edge of its tuning range. At a signal center wavelength of 3.2 μm, we achieve spectral overlap between the second harmonic (SHG) of the SPOPO signal comb and the reference laser, and are able to observe an RF beat $f^{s(\mathrm{SHG})}_{\mathrm{beat}}$ on a photodetector. In a first experiment, we analyze $f^{s(\mathrm{SHG})}_{\mathrm{beat}}$ using a Fourier transform (FFT) analyzer to study the residual SPOPO comb tooth linewidth. The results are shown in Fig. 3. For short acquisition times of less than a millisecond, the SHG comb linewidth is about 50 kHz. On longer timescales, the linewidth broadens to about 150 kHz, much greater than the 3 kHz linewidth of the pump. This can be explained by SPOPO cavity length fluctuations caused by

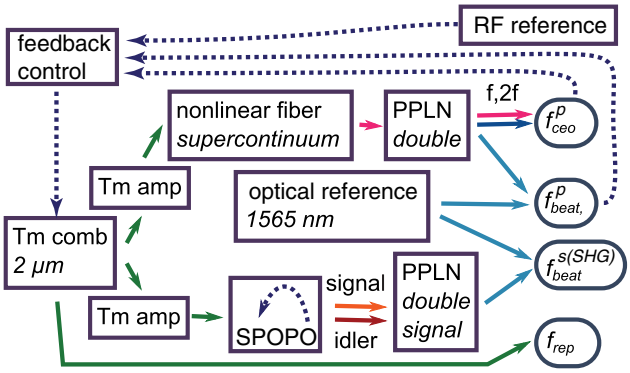

Fig. 2. (Color online) Schematic of the laser and locking feedback, showing the sources of measured frequencies. Solid arrows indicate light beams, dashed lines indicate electronic feedback.

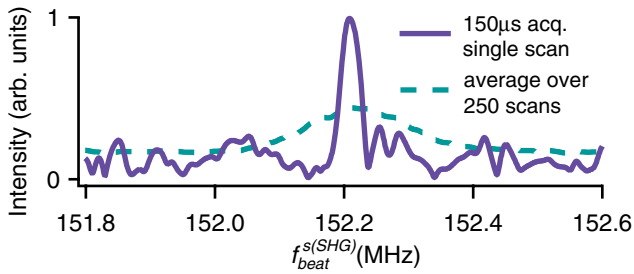

Fig. 3. (Color online) Beat frequency between the frequency-doubled SPOPO signal wave and reference diode laser (which appears twice every f_{rep}). The solid line is a single acquisition from an FFT analyzer over 150 μs, the dashed line is an average of 250 acquisitions. Both curves are normalized to the peak of the 150 μs scan.

the cavity dithering, imperfect locking and acoustic noise.

For a more detailed analysis, we count the frequencies $f_{\mathrm{rep}}, f^{p}_{\mathrm{ceo}}, f^{p}_{\mathrm{beat}}$, and $f^{s(\mathrm{SHG})}_{\mathrm{beat}}$ as shown on the right side of Fig. 2. For counting of $f^{s(\mathrm{SHG})}_{\mathrm{beat}}$ we used an RF-transfer oscillator. Using the comb equation for pump laser and frequency-doubled SPOPO signal comb, we can write ν_{ref} as $\nu_{\mathrm{ref}} = n_{\mathrm{ref}} \cdot f_{\mathrm{rep}} \pm f^{p}_{\mathrm{ceo}} \pm f^{p}_{\mathrm{beat}}$ and $\nu_{\mathrm{ref}} = m_{\mathrm{ref}} \cdot f_{\mathrm{rep}} \pm 2 f^{s}_{\mathrm{ceo}} \pm f^{s(\mathrm{SHG})}_{\mathrm{beat}}$. Here, the integer m_{ref} indicates the SHG comb tooth, which beats with the reference laser.

By equating these two expressions for ν_{ref}, we get an expression for the CEO of the SPOPO signal in terms of measured quantities: $\pm f^{s}_{\mathrm{ceo}} = ((n_{\mathrm{ref}} - m_{\mathrm{ref}}) f_{\mathrm{rep}} \pm f^{p}_{\mathrm{ceo}} \pm f^{p}_{\mathrm{beat}} \mp f^{s(\mathrm{SHG})}_{\mathrm{beat}})/2$. Thus, the signal field is characterized to within the unknown signs and $(n_{\mathrm{ref}} - m_{\mathrm{ref}})$ value. Figure 4 shows f^{s}_{ceo} as calculated from the counter values over 3 h with 1 s gate time. We find that f^{s}_{ceo} is not random but stays within 10 kHz on 10 min timescales and within ~200 kHz over 3 h and the fluctuations are mainly caused by drifts of the reference laser.

We also observed that a change of f^{s}_{ceo} is a linear function of a change of f^{p}_{ceo} over at least a 3 MHz range, as plotted in Fig. 5. When calculating f^{s}_{ceo}, the ± signs and the $n_{\mathrm{ref}} - m_{\mathrm{ref}}$ terms are unknown, but all possible permutations result in a slope of either 0.631 or 1-0.631. Figure 5 shows data for the variation of f^{s}_{ceo} with f^{p}_{ceo}, where all ± signs are taken as positive, and $(n_{\mathrm{ref}} - m_{\mathrm{ref}})$ is taken as –1, giving a slope of 0.631.

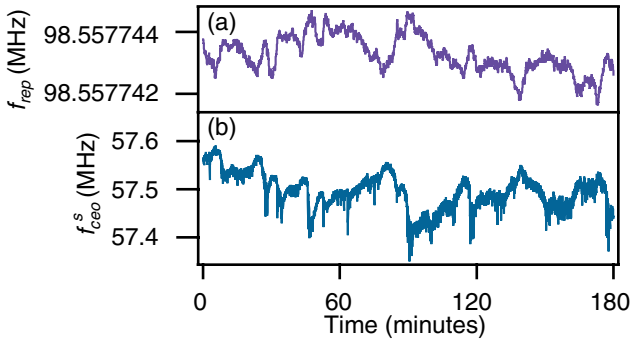

Fig. 4. (Color online) Drift of (a) f_{rep} and (b) f^{s}_{ceo} measured over 3 h. Drifting of the reference laser directly causes drifting of f_{rep} and consequently drifts in f^{s}_{ceo}.

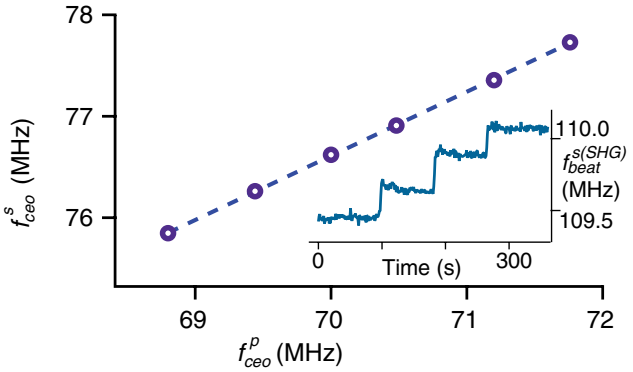

Fig. 5. (Color online) f^s_{ceo} as a function of f^p_{ceo}. The dashed line is a fit using a slope of 0.631. Inset: Example of measured response of $f^{s(\mathrm{SHG})}_{\mathrm{beat}}$ as f^p_{ceo} is stepped.

To understand the slope, consider the change of f^p_{ceo} by $\Delta f^p_{\mathrm{ceo}}$. The signal and idler frequency of each SPOPO comb tooth will then change because of photon energy conservation. The feedback loop will then react and readjust the SPOPO cavity length such that both signal and idler combs are again in resonance. The corresponding cavity resonance conditions for cavity modes close to the center of the signal and idler bands are, respectively, $k^s_q L + k'^s_q l = 2\pi q$ and $k^i_r L + k'^i_r l = 2\pi r$. Here, k is a wave vector in free-space (purged air, nearly dispersion-free), k' is a wave vector in the dispersive material (crystal, CaF_2 wedge), q and r are the integers, and L and l are the lengths of the free-space cavity path, and dispersive material path. We ignore the mirror dispersion which is small here. The cavity length feedback loop changes the dispersion-free cavity length by ΔL.

By differentiating the two resonance conditions with respect to L, omitting mode indices q and r for signal and idler, and noting that $dk/d\nu = 2\pi c^{-1}$ and $dk'/d\nu = 2\pi n_g c^{-1}$, where n_g is the group velocity in the crystal, ν is the frequency, and c is the speed of light, we get $\Delta\nu_{s,i}/\nu_{s,i} = -\Delta L/(L + n_{g,(s,i)} l)$. The ratio $\Delta L/(L + n_g l)$ is the same for signal and idler to within 10^{-5}, therefore $\Delta\nu_s/\Delta\nu_i \approx \nu_s/\nu_i$, i.e., since the number of cavity waves stays constant, the signal and idler frequencies change in proportion to their absolute values.

The change in signal and idler frequency will be distributed according to the comb equations: $\Delta\nu_{s,i} = n_{s,i}\Delta f_{\mathrm{rep}} + \Delta f^{s,i}_{\mathrm{ceo}}$, where $n_{s,i}$ are the corresponding signal and idler comb tooth numbers. Expansion of the equation for f_{rep} for a change in f^p_{ceo} yields $\Delta f_{\mathrm{rep}} = \pm\Delta f^p_{\mathrm{ceo}}/n_{\mathrm{ref}}$. Approximating $n_{s,i}/n_{\mathrm{ref}} \approx \nu_{s,i}/\nu_{\mathrm{ref}}$ we get $\Delta f^s_{\mathrm{ceo}}/\Delta f^i_{\mathrm{ceo}} \approx \nu_s/\nu_i$. Since $\nu_s + \nu_i = \nu_p$, a simple calculation gives $\Delta f^s_{\mathrm{ceo}}/\Delta f^p_{\mathrm{ceo}} \approx \nu_s/\nu_p$. If we insert the center-of-mass wavelengths of our measured spectra, we get $\nu_s/\nu_p = (2.0\ \mu\mathrm{m})/(3.2\ \mu\mathrm{m}) = 0.63$. Taking the center signal (or idler) frequency is an approximation; for an exact calculation, the SPOPO cavity dispersion and the dither lock's lock-point need to be known. In different experiments we observed slopes from 0.61 to 0.64.

We conclude that the offset frequencies of the signal and idler comb from a doubly resonant, SPOPO do not wander randomly, but vary linearly as we vary the offset frequency of the pump. The slope is approximately given by the signal (or idler) to pump center-frequency ratio, a consequence of maintaining the double resonance condition for signal and idler. Our SPOPO's comb linewidth is less than 200 kHz, limited by the dither-lock technique and acoustic noise. Our observed tuning range is from 3 to 6 μm. This can be extended to the 17 μm transparency cutoff of GaAs by using appropriate mirror reflectivities and GaAs reversal periods. Given their broad wavelength tuning range, low pump threshold (~20 mW), and high degree of coherence, nondegenerate, doubly resonant SPOPOs are a promising light source for comb spectroscopy in the entire molecular fingerprint region.

References

1. S. T. Cundiff and J. Ye, Rev. Mod. Phys. **75**, 325 (2003).
2. A. Foltynowicz, P. Maslowski, T. Ban, F. Adler, K. C. Cossel, T. C. Briles, and J. Ye, Faraday Disc. Chem. Soc. **150**, 23 (2011).
3. M. Vainio, M. Merimaa, and L. Halonen, Opt. Lett. **36**, 4122 (2011).
4. A. Schliesser, N. Picque, and T. W. Hänsch, Nat. Photonics **6**, 440 (2012).
5. M. K. Oshman and S. E. Harris, IEEE J. Quantum Electron. **4**, 491 (1968).
6. F. Adler, K. C. Cossel, M. J. Thorpe, I. Hartl, M. E. Fermann, and J. Ye, Opt. Lett. **34**, 1330 (2009).
7. N. Leindecker, A. Marandi, R. L. Byer, and K. L. Vodopyanov, Opt. Express **19**, 6296 (2011).
8. R. Gebs, T. Dekorsy, S. A. Diddams, and A. Bartels, Opt. Express **16**, 5397 (2008).
9. T. I. Ferreiro, J. Sun, and D. T. Reid, Opt. Lett. **35**, 1668 (2010).
10. N. Leindecker, A. Marandi, R. L. Byer, K. L. Vodopyanov, J. Jiang, I. Hartl, M. Fermann, and P. G. Schunemann, Opt. Express **20**, 7046 (2012).
11. S. T. Wong, K. L. Vodopyanov, and R. L. Byer, J. Opt. Soc. Am. B **27**, 876 (2010).
12. J. Bethge, J. Jiang, C. Mohr, M. Fermann, and I. Hartl, in *Lasers, Sources, and Related Photonic Devices* (Optical Society of America, 2012), p. AT5A.3.